

Effect of OH groups on the polyamorphic transition of polyol aqueous solutions

Cite as: J. Chem. Phys. 150, 224508 (2019); doi: 10.1063/1.5095649

Submitted: 11 March 2019 • Accepted: 24 May 2019 •

Published Online: 14 June 2019



View Online



Export Citation



CrossMark

Yoshiharu Suzuki^{a)} 

AFFILIATIONS

Research Center for Advanced Measurement and Characterization, National Institute for Materials Science (NIMS), Namiki 1-1, Tsukuba, Ibaraki 305-0044, Japan

Note: This paper is part of a JCP Special Topic on Chemical Physics of Supercooled Water.

^{a)} Author to whom correspondence should be addressed: suzuki.yoshiharu@nims.go.jp. Telephone: +81-29-860-4877.

ABSTRACT

Polyamorphic transition in water is expected to occur at low temperatures and high pressures. Recently, the polyamorphic transitions of polyol aqueous solutions were examined under pressure at low temperatures, and the location of their liquid-liquid critical points was estimated experimentally. The addition of polyol solute in water induces the shift of polyamorphic transition pressure toward the lower pressure side. Here, by comparing the polyamorphic transition of various polyol aqueous solutions, especially by comparing those of dilute 1,2-propanediol and dilute 1,3-propanediol aqueous solutions, it is clarified that the OH-groups in the polyol molecule efficiently affect the polyamorphic behavior of solvent water. This suggests that the hydrogen bonding interaction between solvent water and polyol solute relates closely to the polyamorphic behavior of solvent water such as the stabilization of high-density-amorph-like solvent water induced by the presence of polyol solute. In addition, the effect of CH₃ groups in the 1,2-propanediol molecule seems to be opposite to the effect of OH groups. These results have important implications for the understandings of low-temperature phenomena of aqueous solutions, for example, hydration, segregation, phase separation, folding/unfolding of macromolecules, glass forming, and nucleation of crystalline ice Ih.

Published under license by AIP Publishing. <https://doi.org/10.1063/1.5095649>

I. INTRODUCTION

Liquid water can be vitrified at low temperatures without crystallization. The vitrification process of water requires extraordinary high cooling rates.^{1,2} Strangely, there are two glassy waters, low-density amorph (LDA) and high-density amorph (HDA), with different densities.^{3,4} The LDA and HDA exist in the low and high pressure regions, respectively. The LDA and HDA undergo a discontinuous transition to each other due to the changes in pressure and temperature.^{4,5} It is thought that the LDA and HDA have different glass transition temperatures.⁶ The experimental findings obtained from experiments of supercooled water and two water amorphs strongly suggest that there are two different liquids, low-density liquid (LDL) and high-density liquid (HDL), corresponding to LDA and HDA, respectively.⁷⁻¹⁰ Moreover, they predict the existence of a liquid-liquid critical point (LLCP) relating to the two liquid waters. However, there is no definitive experimental evidence showing the existence of LLCP. This is because the

temperature-pressure region in which the LLCP is expected to exist is the metastable region of liquid water, and the liquid water crystallizes rapidly. Since the appearance of LDL near the LLCP may promote the crystallization,¹¹⁻¹⁴ the direct observation of LLCP may be practically impossible.¹⁵ On the other hand, the experimental results obtained from the measurable supercooled water around the LLCP and the LDA and HDA near the glass transition temperatures strongly suggest the existence of LLCP,^{6,16-21} although they are pieces of indirect evidence. Computer simulation studies using water potential models of TIP4P/2005 and ST2 show that LDL and HDL can coexist and that the LLCP exists.^{7,22-26} The experimental study by Mishima¹⁸ and the theoretical study by Holten *et al.*²⁷ have proposed that the location of LLCP of water exists at ~223 K and ~0.05 GPa.

According to the general critical phenomenon, the dynamic fluctuation of the two states increases in the vicinity of a critical point and then diverges at the critical point. If the LLCP of water exists, it is expected that the fluctuation between LDL and

TABLE I. Molecular structure of EG, PD₁₃, PD₁₂, and GL.

Solute	Abbreviation	Molecular structure	Number of OH groups	Number of carbon atoms	Number of CH ₃ groups
Ethylene glycol	EG		2	2	0
1,3-propanediol	PD ₁₃		2	3	0
1,2-propanediol	PD ₁₂		2	3	1
Glycerol	GL		3	3	0

HDL becomes large near the LLC. It is believed that the influence of fluctuation spreads around 1 atm and causes anomalous behaviors of the low-temperature and low-pressure liquid water. In other words, when high-temperature water at 1 atm is cooled, the high-temperature water characterized by the HDL transforms into the low-temperature water characterized by the LDL across the supercritical regions relating to the LLC of water. The anomalous behavior may occur during the LDL-HDL crossover.

I know that there are several ideas besides the LLC hypothesis that explain the behavior of supercooled water.^{15,28–30} In this paper, assuming that the LLC hypothesis is plausible, I will discuss the state of solvent water in the dilute polyol aqueous solutions based on the LLC hypothesis.

The idea that the fluctuation between two liquid states around the LLC affects the behavior of pure water can be applied to the aqueous solution system. In the previous studies,^{31–33} we have shown that the polyamorphic transition of the dilute glycerol aqueous solution occurs relating to the LDA-HDA transition of pure water, and the state of the solvent water in glycerol aqueous solution is classified into LDA-like and HDA-like states. This transition between the LDA-like and HDA-like solvent water has hysteresis and hardly depend on the temperature history (see the [supplementary material](#)). As the solute concentration decreases, the behavior of solvent water approaches the polymorphic behavior of pure water. The polymorphic behavior of the dilute aqueous solution is consistent with the LLC hypothesis of water. This suggests that the LLC hypothesis developed for pure water is applicable for the aqueous solution.

On the other hand, in contrast to the effect of solute on the polyamorphic behavior of solvent water, it has been reported that the polyamorphic change of solvent water affects the dynamical structure of the solute molecule.^{34,35} So far, there are several research reports on the structure and behavior of the solvent water in aqueous solution which is considered from the viewpoint of the LLC hypothesis of water.^{11,31–55} However, the study on the polyamorphism of aqueous solutions has only just begun, and the relationship between the solute and polyamorphic solvent water, in particular, the interaction between the solute and LDL (or HDL), is little understood.

In the previous studies,^{31–33} the polyamorphic transitions of ethylene glycol (EG), glycerol (GL), *meso*-erythritol (ER), xylitol (XY), and D-sorbitol (SO) aqueous solutions under high pressure and their solute concentration dependences have been examined. The addition of polyol solute shows a tendency to shift the

equilibrium transition pressure toward the lower pressure side. The shift of transition pressure becomes larger in the order of EG, GL, ER, XY, and SO. Here, when these transition pressures are plotted against the concentration of the number of OH groups (or carbon atoms) in a solute molecule, the solute nature dependence of the equilibrium transition pressure seems to disappear.³³ However, from this result, it is difficult to reveal whether OH groups in the polyol molecule, or carbon sites in the polyol molecule, affect the polyamorphic behavior of solvent water.

In this study, to clarify which site in a polyol molecule affects the polyamorphic behavior of the solvent water, the polyamorphic transitions of 1,3-propanediol (PD₁₃) aqueous solution and of 1,2-propanediol (PD₁₂) aqueous solution are examined and their polyamorphic behaviors are compared with the polyamorphic behaviors of the EG and GL aqueous solutions in the previous studies. The PD₁₃ and PD₁₂ are isomer, and they have three carbon atoms and two OH groups. Their molecular structure is different as shown in [Table I](#). In addition, the PD₁₂ molecules are assumed to have more hydrophobic nature than the PD₁₃ molecule because the PD₁₂ molecule has one CH₃ group, and the PD₁₃ molecule has no CH₃ group.

As shown in [Table I](#), the number of OH groups in a PD₁₂ molecule and a PD₁₃ molecule is the same as the number of OH groups in an EG molecule. The number of carbon atoms in a PD₁₂ molecule and a PD₁₃ molecule is the same as the number of carbon atoms in a GL molecule. If the OH groups in a solute molecule contribute to the polyamorphic behavior of solvent water, the polyamorphic behavior of the PD₁₃ and PD₁₂ aqueous solutions will be similar to the polyamorphic behavior of the EG aqueous solution. If the carbon sites in a solute molecule contribute to the polyamorphic behavior, the polyamorphic behavior of the PD₁₃ and PD₁₂ aqueous solutions will be similar to the polyamorphic behavior of the GL aqueous solution. In this paper, I will discuss the effects of OH groups and carbon sites in the polyol solute on the polyamorphic transition of solvent water.

II. SAMPLE AND EXPERIMENTAL METHODS

A. Preparation of solution sample

PD₁₃ and PD₁₂ were purchased from Wako Pure Chemical Industries Ltd. Each polyol substance was mixed with high-purity H₂O (Millipore: Direct-Q UV). The solute concentration, x , is in the range of 0.03–0.15, where the x stands for the solute molar fraction

which is a ratio of solute molar number to the sum of solute molar number and water molar number.

In order to hinder the crystallization of the dilute aqueous solution, the aqueous solutions were emulsified. The emulsion sample was made by high-speed blending the 1 g of sample solution and a matrix (0.75 g of methylcyclohexane, 0.75 g of methylcyclopentane, and 50 mg of sorbitan tristearate) for 1 min using a homogenizer (OMNI International: Omni TH) with 30 000 rpm. The emulsion size is 1–10 μm in diameter. In order to compare the present experimental results with the previous results of polyol aqueous solutions and pure water,^{31–35} the same emulsification procedure was used. The influence of emulsification procedure on the polyamorphic behavior of pure water and aqueous solution has been reported by Hauptmann *et al.*⁵⁶ According to their report, the emulsification procedure in this study little influences the freezing and transition of aqueous solutions.

B. Pressure apparatus

A piston-cylinder high-pressure apparatus and an indium container were used for the high-pressure experiment and for the preparation of a high-density glassy sample. The cylinder temperature, T_{cy} , was measured by an alumel-chromel thermocouple attached on the cylinder and was controlled by the balance of the attached heater and atmosphere of cold nitrogen gas. The volume of the indium container with the emulsified sample was calculated from the change of the piston displacement with the change in pressure. The error of pressure, caused by the friction between piston and cylinder, was corrected by using the compression and decompression curves of the indium container without sample that were obtained in the same experimental condition. The evaluation of the pressure correction has been described in Ref. 32.

C. Preparation of high-density glassy sample for the measurement of specific volume

In general, when cooling a dilute aqueous solution at 1 atm, a part of solvent water crystallizes to ice Ih and then the segregation to the water-rich crystalline part and the solute-rich glassy part occurs. The concentration inhomogeneity in the aqueous solution complicates the analysis of polyamorphic transition. In order to enable the examination of the polyamorphic behavior of the dilute aqueous solution, it is necessary to prepare the glassy sample in which the solute molecules disperse homogeneously.

In order to prepare a homogeneous high-density glassy sample consisting of the HDA-like solvent water as the starting sample, the dilute polyol aqueous solution was compressed at 0.3 GPa at room temperature and then the aqueous solution was rapidly cooled down to 77 K at a cooling rate of ~ 40 K/min (Fig. 1). Previously, we have vitrified the emulsified pure water² and the bulky dilute aqueous solution, such as LiCl aqueous solution^{53,57} and several polyol aqueous solution,^{31–33} by a rapid cooling under pressure and then examined the state of the glassy water and glassy solvent water. The glassy state of water relates closely to the state of HDA.^{2,32,53}

In this study, about 1.5 ml of the fresh emulsified sample was sealed in the indium container at 1 atm, compressed to 0.3 GPa at room temperature by using the piston-cylinder apparatus, and then cooled to 77 K (Fig. 1). The PD₁₃ and PD₁₂ aqueous solutions below $x = 0.02$ crystallized. Therefore, I examined the

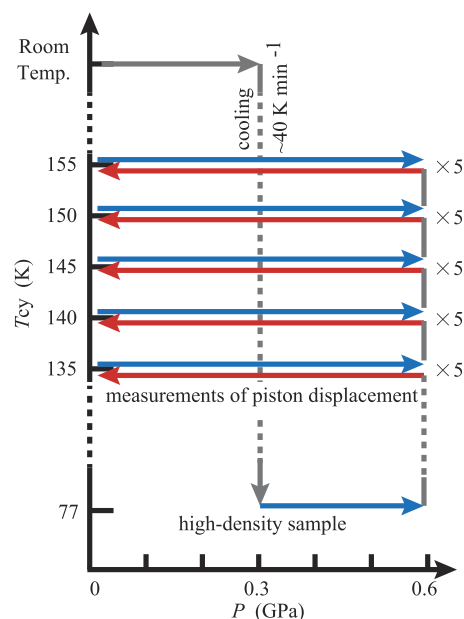


FIG. 1. Temperature-pressure steps for the preparation of the high-density glassy sample and for the measurement of polyamorphic transition.

polyamorphic transition of the PD₁₃ and PD₁₂ aqueous solutions above $x = 0.03$. Previously, we have measured the change in the sample temperature during the cooling process and verified that there is no exothermic event caused by the crystallization of solvent water. I have also checked using Raman spectroscopy that the sample made by the high-pressure cooling process without the exothermic event contains no crystalline parts.³² Moreover, in the previous study for the high-density glassy glycerol aqueous solution made by the same preparation condition,^{31–33} it is found that the glycerol solutes disperse homogeneously because of the good reproducibility of repetitive polyamorphic transition; suggesting strongly that the high-density glassy sample is a homogeneous glass. The check of the crystallization of the sample using the X-ray diffraction method is desirable, but not done in the study.

D. Measurement of the specific volume

A typical experimental protocol for the measurement of specific volume in this study is shown in Fig. 1. The high-density glassy sample made by cooling at 0.3 GPa was further compressed to 0.6 GPa at 77 K, and the piston-cylinder with the sample was heated to a given T_{cy} . The sample at the T_{cy} was decompressed from 0.6 to 0.01 GPa, kept at 0.01 GPa for about 2 min, and then compressed to 0.6 GPa. During the decompression and compression processes, the change in the piston displacement, d , was measured. This measurement was repeated five times at the same T_{cy} . The T_{cy} was changed in the order of 135, 140, 145, 150, and 155 K, as shown in Fig. 1. The decompression rate and compression rate may affect the experimental results of the polyamorphic behavior such as the transition pressure. Therefore, the decompression rate and compression rate in this experiment were fixed at ~ 1.6 MPa/s which was the same as the rate used in the previous studies.^{31–33} The effect of the change of

sample temperature caused by the polyamorphic transition on the T_{cy} is little because the amount of sample is remarkably less than of the piston-cylinder.

The specific volume of the aqueous solution was calculated by subtracting the volume of the indium container and the volume of the emulsion matrix from the measured volume. Here, the pressure and temperature effects, such as the compressibility and thermal expansion, on the volume of the indium container and the volume of the emulsion matrix are considered. For example, the compression and decompression curves of the indium container at 135, 140, 145, 150, and 155 K were measured in advance. In addition, the pressure dependences of the specific volume of the emulsion matrix at 135, 140, 145, 150, and 155 K in the compression and decompression processes were measured in advance. The specific volume of the sample was calculated using this information considering the pressure and temperature effects. We have verified that there is no transition of the indium container between 0.001 and 0.6 GPa and there is no transition of the emulsion matrix.³² The error of the absolute value of specific volume is estimated to be $\pm 2\%$.

The five times average of the compression curve, V_c , and the five times average of the decompression curve, V_d , of specific volume for the PD₁₃ aqueous solutions at 145 K and PD₁₂ aqueous solutions at 150 K are shown in Fig. 2. The glassy sample at the higher T_{cy} crystallizes during or after the polyamorphic transition in the decompression process. The crystallized sample can be checked by the compression curve which does not have the stepwise volume change relating to the polyamorphic transition. The crystallized sample was not used.

E. Analysis method

Figures 2(a) and 2(b) show the V_c and V_d for the PD₁₃ aqueous solutions at 145 K and PD₁₂ aqueous solutions at 150 K,

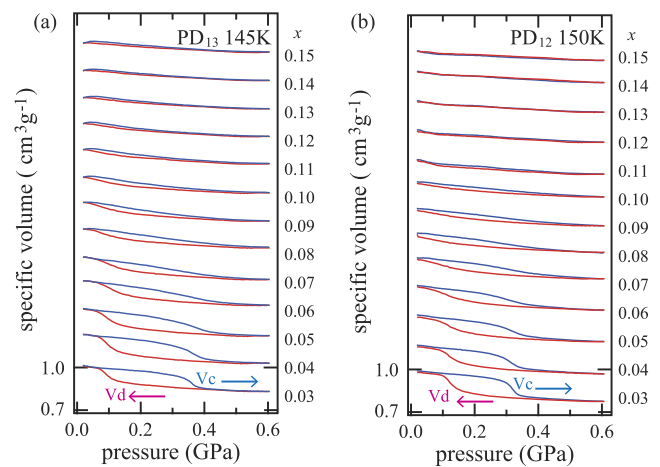


FIG. 2. The compression and decompression curves of specific volume for the PD₁₃ and PD₁₂ aqueous solutions. (a) The compression and decompression curves (V_c and V_d , respectively) of specific volume for the PD₁₃ aqueous solutions of $x = 0.03$ – 0.15 at 145 K were measured in the pressure range between 0.01 and 0.60 GPa. The V_c and V_d are presented by blue and red, respectively. The V_c and V_d except for ones of $x = 0.03$ are shifted vertically for clarity. (b) The V_c and V_d of specific volume for the PD₁₂ aqueous solutions of $x = 0.03$ – 0.15 at 150 K were measured in the pressure range between 0.01 and 0.60 GPa.

respectively. It is difficult to determine the starting and ending pressures of polyamorphic transitions accurately from the stepwise change of V_c and V_d . In order to discuss the polyamorphic transition more quantitatively, I introduced a new parameter, $\Delta V = (V_c - V_d)/V_{c=0.01\text{GPa}}$, where $V_{c=0.01\text{GPa}}$ stands for the V_c at 0.01 GPa.³¹ Figures 3(a) and 3(d) show the ΔV for the PD₁₃ aqueous solutions and PD₁₂ aqueous solutions, respectively.

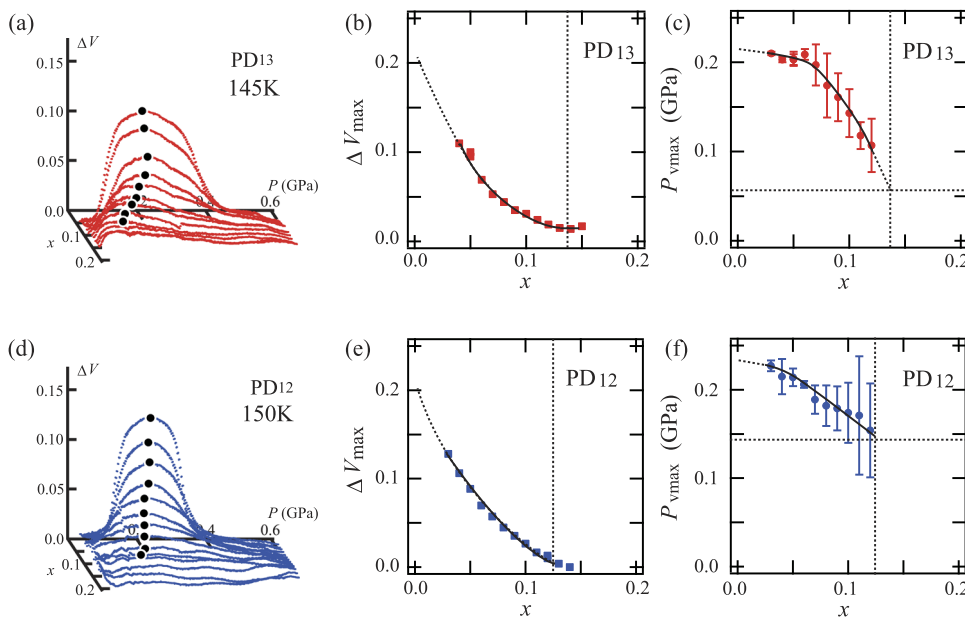


FIG. 3. Analysis results of polyamorphic transition for the PD₁₃ and PD₁₂ aqueous solutions. (a)–(c) are the x dependence of ΔV , the x dependence of ΔV_{\max} , and the x dependence of $P_{V_{\max}}$ for the PD₁₃ aqueous solution at 145 K, respectively. (d)–(f) are the x dependence of ΔV , the x dependence of ΔV_{\max} , and the x dependence of $P_{V_{\max}}$ for the PD₁₂ aqueous solution at 150 K, respectively. The solid curve and the dashed curve in (b), (c), (e), and (f) are the fitted curve and the extrapolated curve, respectively. The vertical dashed line in (b) and (e) stands for the value of x_{LLCP} . The horizontal dashed line in (c) and (f) stands for the value of P_{LLCP} . The crossing point of the vertical and horizontal dashed lines may be the LLCP location for the PD₁₃ aqueous solutions at 145 K and the PD₁₂ aqueous solutions at 150 K. The error bars of ΔV_{\max} are small and are hidden behind the square mark.

these solutions in the low x region has a dome-type part indicating that the polyamorphic transition occurs. The shape of dome part characterizes the behavior of polyamorphic transition. The maximum value of the dome part of ΔV , ΔV_{\max} , corresponds to the gap of stepwise polyamorphic transition and indicates a volume ratio of the low-density sample and the high-density sample. Indeed, the ΔV_{\max} calculated from the LDA-HDA transition of pure water at ~ 135 K is about 0.2³¹ and agrees with the volume ratio of LDA and HDA reported by Mishima *et al.*^{4,5}

The pressure of ΔV_{\max} , $P_{V_{\max}}$, indicates the equilibrium pressure of polyamorphic transition, and the x dependence of $P_{V_{\max}}$ relates to the equilibrium coexistent line of low-density and high-density states, the so-called liquid-liquid transition (LLT) line. The dome part of ΔV is quite asymmetric, and the $P_{V_{\max}}$ is different from the pressure previously defined by the middle point between the pressure of polyamorphic transition from the low-density to high-density state and the pressure of polyamorphic transition from the high-density to low-density state.^{32,33} Therefore, the $P_{V_{\max}}$ may not be the correct pressure of equilibrium LLT.

III. EXPERIMENTAL RESULTS

A. Polyamorphic behavior of PD₁₃ aqueous solution

The specific volume changes of PD₁₃ aqueous solution at 145 K during the compression and decompression processes are shown in Fig. 2(a). The x dependences of ΔV , ΔV_{\max} , and $P_{V_{\max}}$, which are calculated from the analysis of V_c and V_d , are shown in Figs. 3(a), 3(b), and 3(c), respectively. As the x increases, the dome part of ΔV is collapsed, the height of the dome part is lowered, and the shape of ΔV becomes flat eventually. The x at which the shape of ΔV begins to be flat is estimated from Fig. 3(b). The ΔV_{\max} corresponding to the height of the dome part decreases continuously with the increase of x , the ΔV_{\max} becomes almost zero at $x \sim 0.140$, and then the change of ΔV_{\max} becomes constant above $x \sim 0.140$. This indicates that the polyamorphic transition disappears around $x \sim 0.140$. Therefore, the x_{LLCP} of PD₁₃ aqueous solution at 145 K is 0.140 ± 0.005 .

The $P_{V_{\max}}$ decreases, as the x increases, as shown in Fig. 3(c). This indicates that the pressure of polyamorphic transition becomes

lower by the addition of solute. From the x dependence of $P_{V_{\max}}$ in Fig. 3(c), I estimate that the transition pressure at $x_{\text{LLCP}} = \sim 0.140$ is ~ 0.055 GPa. I estimate that the LLCP of the PD₁₃ aqueous solution of 145 K is located at $P_{\text{LLCP}} = 0.055 \pm 0.005$ GPa at $x_{\text{LLCP}} = 0.140 \pm 0.005$.

The value of ΔV_{\max} extrapolated to $x = 0$ in Fig. 3(b) is about 0.2. This value is equal to ΔV_{\max} (~ 0.2) estimated from the LDA-HDA transition of pure water at 135 K³¹ and is consistent with the volume ratio of LDA and HDA.^{4,5}

The value of $P_{V_{\max}}$ extrapolated to $x = 0$ in Fig. 3(c) is about 0.23 GPa. This value agrees with the results obtained from other polyol aqueous solutions in the previous study that the $P_{V_{\max}}$ at $x = 0$ is ~ 0.23 GPa.³¹ This value corresponds to the pressure of the equilibrium LDA-HDA boundary that is the pressure of the LLT line. The value is slightly larger than the value of ~ 0.2 GPa which is proposed by Mishima *et al.*^{4,5}

From a viewpoint of the water polyamorphism, the schematic P - T - x diagram of the polyamorphic state of solvent water in the PD₁₃ aqueous solution as shown in Fig. 4(a) is considered. The LLT line in the P - x plain at 145 K is the $P_{V_{\max}}$ - x curve estimated in this study. The LLT line of pure water and the LLCP in the T - P plain are referred from works by Mishima¹⁸ and Holten *et al.*²⁷ Figure 4(a) shows that the solvent state in the lower pressure region than the LLT line is the LDA-like state and the solvent state in the higher pressure region than the LLT line is the HDA-like state. This suggests that the state of solvent water in the PD₁₃ aqueous solution is classified into the two polyamorphic states, LDA-like and HDA-like states. This is consistent with the previous results that the solvent water in the other aqueous solutions such as polyol and lithium-chloride aqueous solutions is characterized by the LDA-like and HDA-like waters.^{31,32,53}

B. Polyamorphic behavior of PD₁₂ aqueous solution

The specific volume change of PD₁₂ aqueous solution at 150 K during the compression and decompression processes is shown in Fig. 2(b). The x dependences of ΔV , ΔV_{\max} , and $P_{V_{\max}}$ for the PD₁₂ aqueous solution at 150 K are shown in Figs. 3(d), 3(e), and 3(f), respectively. As the x increases, the dome part of ΔV is collapsed, the height of the dome part is lowered, and the shape of ΔV becomes flat

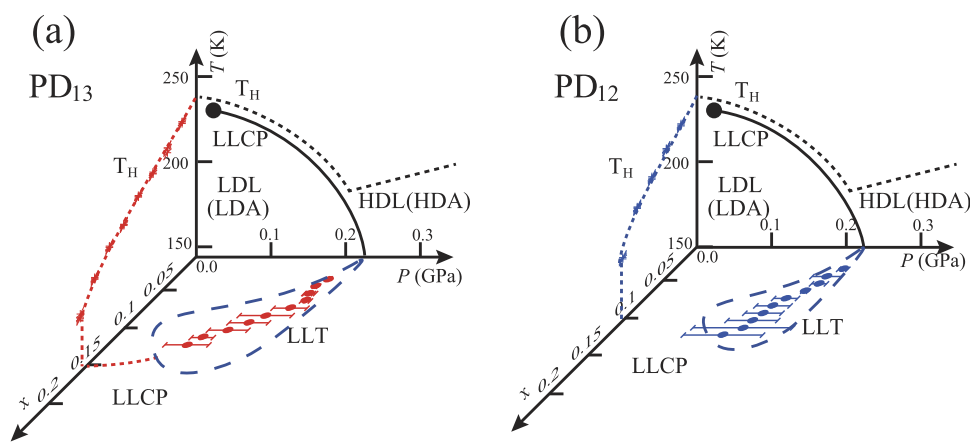


FIG. 4. The schematic P - T - x diagrams of the solvent water in the PD₁₃ and PD₁₂ aqueous solutions considered from a viewpoint of water polyamorphism. (a) and (b) are the P - T - x diagram for the PD₁₃ and PD₁₂ aqueous solutions, respectively. The T_H on the T - x plane is the nucleation temperature of the PD₁₃ and PD₁₂ aqueous solutions at 1 atm. The T_H curve becomes perpendicular to the x axis at x_{TH} . The LLCP and the LLT line estimated in this study are drawn in the P - x plane. The region drawn by the dashed curve on the P - x plane stands for the speculated coexistence region of LDA-like and HDA-like solvent waters.

eventually. The x at which the shape of ΔV begins to be flat is estimated from the change of ΔV_{\max} in Fig. 3(e). The ΔV_{\max} becomes almost zero at $x \sim 0.120$, and then the change of ΔV_{\max} becomes constant above $x \sim 0.120$. This indicates that the polyamorphic transition disappears around $x \sim 0.120$. Therefore, the x_{LLCP} of the PD₁₂ aqueous solution at 150 K is 0.120 ± 0.005 .

From the x dependence of $P_{V_{\max}}$ in Fig. 3(f), it is estimated that the value of $P_{V_{\max}}$ at $x_{\text{LLCP}} \sim 0.120$ is about 0.145 GPa. As a result, I estimate that the LLCP for the PD₁₂ aqueous solution of 150 K is located at $P_{\text{LLCP}} = 0.145 \pm 0.005$ GPa at $x_{\text{LLCP}} = 0.120 \pm 0.005$.

The value of ΔV_{\max} extrapolated to $x = 0$ in Fig. 3(e) is about 0.2. This value agrees with the volume ratio of LDA and HDA, ~ 0.2 .^{4,5} Moreover, the value of $P_{V_{\max}}$ extrapolated to $x = 0$ in Fig. 3(f) is about 0.23 GPa. This value is almost equal to the values estimated from the PD₁₃ aqueous solution in this study and the other polyol aqueous solution in the previous study.^{31,32}

The schematic P - T - x diagram of the polyamorphic state of solvent water in the PD₁₂ aqueous solution as shown in Fig. 4(b) is considered from a viewpoint of the water polyamorphism. The LLT line in the P - x plain at 150 K is a $P_{V_{\max}}$ - x curve estimated in this study. The diagram in Fig. 4(b) suggests that the solvent state in a lower pressure region than the LLT line is the LDA-like state and the solvent state in a higher pressure region than the LLT line is the HDA-like state. As with the classification of solvent water in the PD₁₃ aqueous solution, the state of solvent water in the PD₁₂ aqueous solution can be classified into the two polyamorphic states, LDA-like and HDA-like states.

As shown in Fig. 2, the polyamorphic transition of the aqueous solution is a gradual stepwise volume change and is different from the discontinuous volume change such as the LDA-HDA transition of pure water.³¹ For example, the V_c for the PD₁₃ aqueous solution of $x = 0.04$ in Fig. 2(a) shows that the polyamorphic transition starts around 0.32 GPa and completes around 0.40 GPa. As the x increases, the pressure region in which the polyamorphic transition progresses expands more. This existence of the polyamorphic transition pressure region suggests the appearance of the coexistence region of HDA-like and LDA-like solvent water as shown by the dashed line in Fig. 4. Biddle *et al.*⁴⁵ and Chatterjee *et al.*⁴⁶ have suggested the possibility that the coexistence region of the high-density and low-density states appears during the polyamorphic transition of the aqueous solution. Therefore, the correct transition boundary may be a coexistence region, not a coexistence line. Biddle *et al.*⁴⁵ have proposed that the shape of the coexistence region is the shape as drawn by the dashed line in Figs. 4(a) and 4(b). However, there is no reliable evidence showing the coexistence of the HDA-like state and LDA-like state. It is difficult to evaluate the spread of the coexisting region from this experimental result.

C. Homogeneous nucleation temperature of PD₁₃ and PD₁₂ aqueous solutions at 1 atm

In order to discuss the relation between the homogeneous nucleation and the polyamorphic behavior of PD₁₃ and PD₁₂ aqueous solutions, I measured the homogeneous nucleation temperature, T_H , of the emulsified PD₁₃ and PD₁₂ aqueous solutions at 1 atm. About 10 μl of the emulsified sample was cooled from 300 to 77 K at a cooling rate of ~ 10 K/s, and the change of the sample temperature

during cooling was measured using a tiny alumel-chromel thermocouple. The T_H was determined from the exothermic event due to the crystallization of ice Ih.³³ The x dependences of T_H for the EG, GL, PD₁₃, and PD₁₂ aqueous solutions at 1 atm are shown in Fig. 5. The T_H of the EG and GL aqueous solutions has been measured in the previous study.³³

The T_H decreases with the increase of x . When the x reaches x_{TH} , the aqueous solution does not crystallize and becomes homogeneous glass. The x_{TH} as well as T_H depends on the cooling rate. In the case of this study, the x_{TH} of the PD₁₃ and PD₁₂ aqueous solutions are ~ 0.165 and ~ 0.105 , respectively.

The T_H - x curves for the PD₁₃ and PD₁₂ aqueous solutions are drawn on the T - x plain at 1 atm in Figs. 4(a) and 4(b), respectively. Each x_{TH} seems to be located near each x_{LLCP} . This indicates that a region in which the nucleation of crystalline ice Ih occurs agrees with a region in which the LDA-like solvent water exists. This result is consistent with the previous results for EG, GL, ER, XY, and SO aqueous solutions.³¹ This suggests that the formation of the LDA-like hydrogen-bonding network of water relates closely to the nucleation of crystalline ice Ih.¹¹⁻¹⁴

D. Solute nature dependence of $P_{V_{\max}}$ - x curve for polyol aqueous solution

In Fig. 6(a), the changes of $P_{V_{\max}}$ with the change of x for the PD₁₃ aqueous solution at 145 K and PD₁₂ aqueous solution at 150 K are compared with the previous results for the other polyol aqueous solutions.³¹ The $P_{V_{\max}}$ of EG aqueous solution has been measured at 145 K, and the $P_{V_{\max}}$ of GL, ER, XY, and SO aqueous solutions have been measured at 150 K. The change of $P_{V_{\max}}$ corresponds to the x dependence of the equilibrium polyamorphic transition pressure, and the $P_{V_{\max}}$ - x curve concerns with the equilibrium LLT curve. Each x_{LLCP} of LLCP which is marked by an asterisk in Fig. 6(a) decreases in the order of EG, GL, ER, XY, and SO aqueous solutions, and each $P_{V_{\max}}$ - x curve shrinks to the lower concentration side.

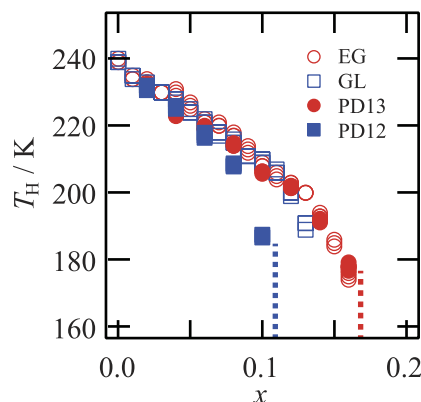


FIG. 5. Concentration dependences of homogeneous nucleation temperature, T_H , of PD₁₃ and PD₁₂ aqueous solutions. The T_H curve becomes perpendicular to the x axis at x_{TH} . The blue and red dashed lines stand for the x_{TH} of PD₁₃ aqueous solutions (~ 0.165) and the x_{TH} of PD₁₂ aqueous solutions (~ 0.105), respectively. The red open circle and blue open square stand for the T_H of EG and GL aqueous solutions, respectively (Ref. 33).

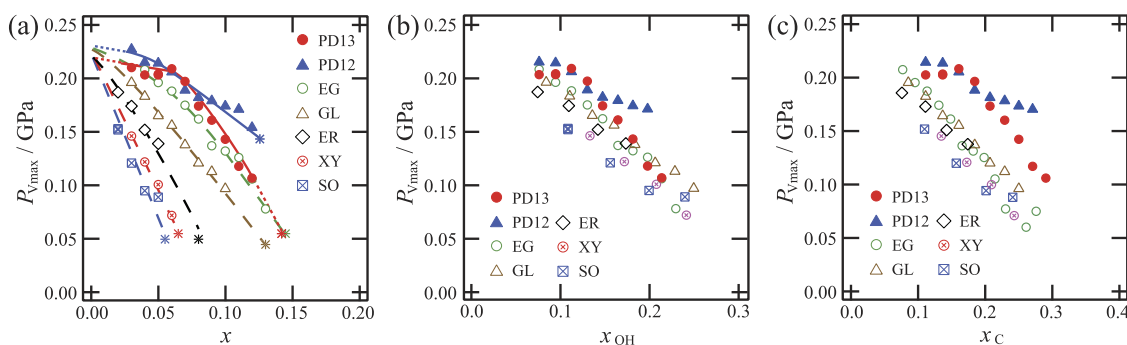


FIG. 6. Concentration dependences of P_{Vmax} for polyol aqueous solutions. (a) The P_{Vmax} is plotted as a function of the solute concentration, x . The asterisk symbol stands for the LLCP. The P_{Vmax} for the EG, GL, ER, XY, and SO aqueous solutions are referred from Ref. 31. (b) The P_{Vmax} is plotted as a function of the concentration of OH groups in the solute molecule, x_{OH} . The number of OH groups in PD₁₃ is the same as that of EG, and the behavior of P_{Vmax} for PD₁₃ aqueous solution is similar to that of EG aqueous solution. (c) The P_{Vmax} is plotted as a function of the concentration of carbon atoms in the solute molecule, x_C . Although the number of carbon atoms in PD₁₃ and PD₁₂ is the same as that of GL, the behavior of P_{Vmax} for PD₁₃ and PD₁₂ aqueous solutions is remarkably different from that of GL aqueous solution.

For example, the P_{Vmax} - x curve of the GL aqueous solution is located on the lower concentration side than the P_{Vmax} - x curve of the EG aqueous solution. The question is which site, OH group site or carbon site, in polyol solute affects the polyamorphic behavior.

The P_{Vmax} - x curve for the PD₁₃ aqueous solution is similar to the P_{Vmax} - x curve of the EG aqueous solution. The slope of the P_{Vmax} - x curve of the PD₁₃ aqueous solution is small below $x = 0.06$, and the slope becomes larger above $x = 0.06$. Above $x = 0.06$, the P_{Vmax} - x curve of the PD₁₃ aqueous solution seems to almost overlap the P_{Vmax} - x curve of the EG aqueous solution. The LLCP location of the PD₁₃ aqueous solution at 145 K ($x_{LLCP} = \sim 0.140$, $P_{LLCP} = 0.055$ GPa) almost agrees with the LLCP location of the EG aqueous solution at 145 K ($x_{LLCP} = \sim 0.145$, $P_{LLCP} = 0.055$ GPa). In addition, the P_{Vmax} - x curve of the PD₁₃ aqueous solution is located in the higher pressure region than the P_{Vmax} - x curve of the GL aqueous solution.

On the other hand, the P_{Vmax} - x curve for the PD₁₂ aqueous solution is different from the P_{Vmax} - x curve for EG aqueous solution. The P_{LLCP} of PD₁₂ aqueous solution (~ 0.145 GPa) is higher than the P_{LLCP} of EG aqueous solution (~ 0.055 GPa), and the P_{Vmax} - x curve of PD₁₂ aqueous solution is located in the higher pressure region than the P_{Vmax} - x curve of EG aqueous solution.

IV. DISCUSSION

The P_{Vmax} - x curve of the polyol aqueous solutions depend on the solute nature as shown in Fig. 6(a). The question is which site, OH group site or carbon site, in the polyol solute affects the difference between the P_{Vmax} - x curves.

In order to clarify the effect of sites in the polyol molecule, the changes of the P_{Vmax} with the change of the concentration x_{OH} that the x is corrected by the number of OH groups are shown in Fig. 6(b). The x_{OH} is defined as the ratio of the number of OH groups to the sum of the number of OH groups and the number of H₂O ($nx/(nx + (1 - x))$), where n is the number of OH groups in a solute molecule. The x_{OH} corresponds to the mole fraction of the OH group in aqueous solution. The changes of the P_{Vmax} with the change of x_{OH} for the EG, GL, ER, XY, and SO aqueous

solutions show almost the same behavior, and these P_{Vmax} - x_{OH} curves overlap at almost the same location. Although the P_{Vmax} - x_{OH} curve of PD₁₃ aqueous solution below $x_{OH} = \sim 0.11$ deviates from the P_{Vmax} - x_{OH} curves of EG, GL, ER, XY, and SO aqueous solutions, the P_{Vmax} - x_{OH} curve of PD₁₃ aqueous solution above $x_{OH} = \sim 0.11$ almost agrees with the P_{Vmax} - x_{OH} curve of other aqueous solutions. On the other hand, the P_{Vmax} - x_{OH} curve of PD₁₂ aqueous solution does not overlap the P_{Vmax} - x_{OH} curve of ER, GL, ER, XY, and SO aqueous solutions.

Next, I show the changes of the P_{Vmax} with the change of the concentration x_C that the x is corrected by the number of carbon atoms in Fig. 6(c). The $x_C (=mx/(mx + (1 - x)))$ corresponds to the mole fraction of carbon atoms, where m is the number of carbon atoms in a solute molecule. The behaviors of P_{Vmax} against the change of x_C for the PD₁₃ and PD₁₂ aqueous solutions clearly differ from those of EG and GL aqueous solutions. The P_{Vmax} - x_C curves of the PD₁₃ and PD₁₂ aqueous solutions are located in the higher pressure side than the P_{Vmax} - x_C curves of the EG and GL aqueous solutions.

The P_{Vmax} - x_{OH} curve of the PD₁₃ aqueous solution is similar to the behavior of P_{Vmax} for the EG, GL, ER, XY, and SO aqueous solutions above $x_{OH} = \sim 0.11$. However, the P_{Vmax} - x_C curve of the PD₁₃ aqueous solution is significantly different from the behaviors of P_{Vmax} for the EG, GL, ER, XY, and SO aqueous solutions. This indicates that as the number of OH groups in a PD₁₃ solute and the number of OH groups in an EG solute are same, the behavior of P_{Vmax} for PD₁₃ aqueous solution is similar to the behavior of P_{Vmax} for EG aqueous solution as shown in Fig. 6(b). However, although the number of carbon atoms in a PD₁₃ solute is the same as that in a GL solute, the behavior of P_{Vmax} for PD₁₃ aqueous solution is remarkably different from that for GL aqueous solution as shown in Fig. 6(c). This result indicates that the OH groups in a solute molecule mainly affect the polyamorphic behavior of solvent water and that the effect of the CH_n site in the solute molecule is weaker than that of OH groups, where the subscript n is 1, 2, or 3. That is, the shift of the polyamorphic transition pressure to the lower pressure side with the increase of x is caused by the presence of OH groups in the solute. This suggests that the hydrogen bonding interaction

between water molecule and solute molecule relates strongly to the polyamorphic behavior of water.

Previous studies on the polyamorphism transition of polyol aqueous solutions^{31–33} have shown that the polyamorphic transition pressure of high-density polyol aqueous solutions in the decompression process becomes lower with the increase of x . This indicates that the HDA-like solvent water in the polyol aqueous solution is stabilized by the addition of polyol solute. In other words, the LDA-like solvent water in the polyol aqueous solution seems to be relatively destabilized by the addition of polyol solute. Signs of the destabilization of the LDA-like sample due to the addition of polyol solute appear in the previous experimental results.^{31,32} For example, the Raman profile of OD-stretching vibration mode in the dilute GL aqueous solution (GL-D₂O system) at 1 atm ($x = 0.07$) is similar to the Raman profile of LDA (pure water), and it is broader than that of LDA. As the x increases, the Raman profile becomes further broad and it approaches the Raman profile of HDA-like solvent water continuously. This indicates that the tetrahedral formation of LDA-like solvent water is distorted by the addition of polyol solute. Moreover, the change of the specific volume of the polyol aqueous solution around 1 atm has shown that the solvent water continuously changes from the LDA state to the HDA state with the increase of x . These experimental findings indicate that the tetrahedral formation of LDA-like solvent water is distorted by the addition of solute and the LDA-like solvent water may be destabilized. Therefore, I conclude from the result of PD₁₃ aqueous solution that the stabilization of HDA-like solvent water and the destabilization of LDA-like solvent water induced by the addition of the polyol molecule are mainly caused by the effect of hydrogen bonding interaction between the OH groups in polyol molecule and water molecule. In order to confirm the conclusion, however, it is necessary in further to examine the effect of OH groups on the polyamorphic behavior of solvent water using a solute except for PD₁₃.

The similar stabilization of HDA-like solvent water in aqueous solution is observed in the lithium chloride (LiCl) aqueous solution system.^{53,54} The effect of the electrostatic interaction between ion and water on the polyamorphic state of water is similar to the effect of the hydrogen bonding interaction between the OH-groups of substance and water. The attractive interaction between substance and water may stabilize the HDA-like water around the substance.

In the case of glassy dilute LiCl aqueous solution, the LiCl solute disperses in HDA-like solvent water homogeneously and does not disperse in LDA-like solvent water.⁵³ When the high-density glassy dilute LiCl aqueous solution is placed in low pressures and high temperatures, the segregation into water-rich LDA and glassy high concentration LiCl aqueous solution occurs. This segregation is thought to be caused by the stabilization of HDA-like water near the LiCl solute. The solute coated by the HDA-like water cannot be dissolved in the LDA-like solvent water and is cooperatively aggregated each other. On the other hand, the polyol molecules can be dispersed homogeneously in LDA-like solvent water. This suggests that the LDA-like water can exist near a polyol molecule. Therefore, the effect of OH groups in the polyol molecule on the stabilization of HDA-like solvent water may be weaker than the effect of LiCl.

Despite the fact that the number of OH groups in a PD₁₂ molecule has the same as the number of OH groups in an EG molecule and in a PD₁₃ molecule, the $P_{V_{\max}-x_{\text{OH}}}$ curve of the PD₁₂

aqueous solution is clearly different from that of the EG and PD₁₃ aqueous solutions as shown in Fig. 6(b). The $P_{V_{\max}-x_{\text{OH}}}$ curve of the PD₁₂ aqueous solution is located in the higher pressure region than that of the PD₁₃ and EG aqueous solutions. Although the PD₁₂ molecule and the PD₁₃ molecule are isomers, the molecular structure of PD₁₂ has high symmetry and the molecular structure of PD₁₂ is asymmetric as shown in Table I. Since the edge site of the PD₁₂ molecule is a CH₃ group, PD₁₂ is assumed to be more hydrophobic than PD₁₃ and GL. Therefore, it is speculated that the anomalous behavior of the $P_{V_{\max}-x_{\text{OH}}}$ curve of the PD₁₂ aqueous solution is caused by the presence of CH₃ groups and that the presence of CH₃ group weakens the effect of OH groups on the polyamorphic behavior. The effect of CH₃ groups may be opposite to the effect of OH groups. In addition, the $P_{V_{\max}-x_{\text{OH}}}$ curve of the PD₁₃ aqueous solution below $x = 0.06$ in Fig. 6(b) resembles that of the PD₁₂ aqueous solution. This may be due to the influence of a hydrophobic CH₂ site at the center of the PD₁₃ molecule. From the experimental results, however, it is premature to conclude the effect of hydrophobic sites, such as the CH_n sites, on the polyamorphic behavior of solvent water. It is necessary to further study on the possible effect of hydrophobic solute, for example, the effects of hydrophobic CH₂ site at the center of the PD₁₃ molecule and the asymmetry of the PD₁₂ molecule, on the polyamorphic behavior of water.

V. SUMMARY

Polyamorphic transitions of the PD₁₂ and PD₁₃ aqueous solutions under high pressure were examined, and their LLCP location was estimated experimentally from the analysis of the x dependence of polyamorphic transition. The information on LLCP for the polyol aqueous solutions in this study is summarized in Table II. The polyamorphic behaviors of PD₁₂ and PD₁₃ aqueous solutions were compared with the previous results of EG, GL, ER, XY, and SO aqueous solutions. The equilibrium polyamorphic pressure ($P_{V_{\max}}$) of the polyol aqueous solutions shifts toward the lower pressure side with the increase of x . This indicates that the HDA-like solvent water is stabilized by the addition of polyol solute in water.

The change of $P_{V_{\max}}$ with the change of x_{OH} corrected by the number of OH groups in a polyol solute suggests that the change of polyamorphic behavior induced by the addition of polyol solute

TABLE II. Location of LLCP for polyol aqueous solutions.^a

Solute	T (K)	x_{LLCP}	P_{LLCP} (GPa)	x_{TH}
PD ₁₃	145	0.140	0.055	0.165
PD ₁₂	150	0.125	0.145	0.105
EG	145	0.145	0.055	0.17
GL	150	0.135	0.045	0.13
ER	150	0.08	0.05	...
XY	150	0.065	0.055	0.11
SO	150	0.055	0.050	0.10

^aThe data in Table I correspond to just one point shown in the P - x plane of Fig. 4. The information on LLCP for EG, GL, ER, XY, and SO aqueous solutions is cited from Ref. 31.

is caused primarily by the OH-groups in the solute. This result suggests that the hydrogen bonding interaction between water molecule and solute molecule greatly relates to the polymorphic behavior of the aqueous solution. Particularly, the hydrogen bonding interaction may stabilize the HDA-like solvent water and may relatively destabilize the LDA-like solvent water. The change in the polymorphic state of solvent water induced by the presence of OH groups may relate closely to the physical, chemical, and biological phenomena in the aqueous solution system such as hydration, segregation, binary phase separation, aggregation, nucleation of ice Ih, glass transition, and glass formation.

SUPPLEMENTARY MATERIAL

The experimental result of the polymorphic transition of dilute GL aqueous solution that does not depend on the temperature history is shown in the [supplementary material](#).

ACKNOWLEDGMENTS

I am grateful to Osamu Mishima for precious discussion and careful review.

REFERENCES

- P. Brüggeller and E. Mayer, *Nature* **288**, 569 (1980).
- O. Mishima and Y. Suzuki, *J. Chem. Phys.* **115**, 4199 (2001).
- O. Mishima, L. D. Calvert, and E. Whalley, *Nature* **310**, 393 (1984).
- O. Mishima, L. D. Calvert, and E. Whalley, *Nature* **314**, 76 (1985).
- O. Mishima, *J. Chem. Phys.* **100**, 5910 (1994).
- K. Amann-Winkel, C. Gainaru, P. H. Handle, M. Seidl, H. Nelson, R. Bohmer, and T. Loerting, *Proc. Natl. Acad. Sci. U. S. A.* **110**, 17720 (2013).
- P. H. Poole, F. Sciortino, U. Essmann, and H. E. Stanley, *Nature* **360**, 324 (1992).
- O. Mishima and H. E. Stanley, *Nature* **396**, 329 (1998).
- P. G. Debenedetti, *J. Phys.: Condens. Matter* **15**, R1669 (2003).
- P. Gallo, K. Amann-Winkel, C. A. Angell, M. A. Anisimov, F. Caupin, C. Chakravarty, E. Lascaris, T. Loerting, A. Z. Panagiotopoulos, J. Russo, J. A. Sellberg, H. E. Stanley, H. Tanaka, C. Vega, L. Xu, and L. G. M. Pettersson, *Chem. Rev.* **116**, 7463 (2016).
- O. Mishima, *J. Chem. Phys.* **123**, 154506 (2005).
- E. B. Moore and V. Molinero, *Nature* **479**, 506 (2011).
- G. Bullock and V. Molinero, *Faraday Discuss.* **167**, 371 (2013).
- R. S. Singh and B. Bagchi, *J. Chem. Phys.* **140**, 164503 (2014).
- K. Binder, *Proc. Natl. Acad. Sci. U. S. A.* **111**, 9374 (2014).
- O. Mishima and H. E. Stanley, *Nature* **392**, 164 (1998).
- O. Mishima, *Phys. Rev. Lett.* **85**, 334 (2000).
- O. Mishima, *J. Chem. Phys.* **133**, 144503 (2010).
- J. A. Sellberg, C. Huang, T. A. McQueen, N. D. Loh, H. Laksmono, D. Schlesinger, R. G. Sierra, D. Nordlund, C. Y. Hampton, D. Starodub, D. P. DePonte, M. Beye, C. Chen, A. V. Martin, A. Barty, K. T. Wikfeldt, T. M. Weiss, C. Caronna, J. Feldkamp, L. B. Skinner, M. M. Seibert, M. Messerschmidt, G. J. Williams, S. Boutet, L. G. M. Pettersson, M. J. Bogan, and A. Nilsson, *Nature* **510**, 381 (2014).
- K. H. Kim, A. Späh, H. Pathak, F. Perakis, D. Mariedahl, K. Amann-Winkel, J. A. Sellberg, J. H. Lee, S. Kim, J. Park, K. H. Nam, T. Katayama, and A. Nilsson, *Science* **358**, 1589 (2017).
- F. Perakis, K. Amann-Winkel, F. Lehmkuhler, M. Sprung, D. Mariedahl, J. A. Sellberg, H. Pathak, A. Späh, F. Cavalca, D. Schlesinger, A. Ricci, A. Jain, B. Massani, F. Aubree, C. J. Benmore, T. Loerting, G. Grübel, L. G. M. Pettersson, and A. Nilsson, *Proc. Natl. Acad. Sci. U. S. A.* **114**, 8193 (2017).
- J. C. Palmer, F. Martelli, Y. Liu, R. Car, A. Z. Panagiotopoulos, and P. G. Debenedetti, *Nature* **510**, 385 (2014).
- R. S. Singh, J. W. Biddle, P. G. Debenedetti, and M. A. Anisimov, *J. Chem. Phys.* **144**, 144504 (2016).
- J. L. F. Abascal and C. Vega, *J. Chem. Phys.* **133**, 234502 (2010).
- T. Sumi and H. Sekino, *RSC Adv.* **3**, 12743 (2013).
- T. Yagasaki, M. Matsumoto, and H. Tanaka, *Phys. Rev. E* **89**, 020301(R) (2014).
- V. Holten, C. E. Bertrand, M. A. Anisimov, and J. V. Sengers, *J. Chem. Phys.* **136**, 094507 (2012).
- R. J. Speedy, *J. Phys. Chem.* **86**, 982 (1982).
- D. T. Limmer and D. Chandler, *Proc. Natl. Acad. Sci. U. S. A.* **111**, 9413 (2014).
- S. Sastry, P. G. Debenedetti, F. Sciortino, and H. E. Stanley, *Phys. Rev. E* **53**, 6144 (1996).
- Y. Suzuki, *J. Chem. Phys.* **149**, 204501 (2018).
- Y. Suzuki and O. Mishima, *J. Chem. Phys.* **141**, 094505 (2014).
- Y. Suzuki, *J. Chem. Phys.* **147**, 064511 (2017).
- Y. Suzuki and O. Mishima, *J. Chem. Phys.* **145**, 024501 (2016).
- C. U. Kim, M. W. Tate, and S. M. Gruner, *Proc. Natl. Acad. Sci. U. S. A.* **108**, 20897 (2011).
- Y. Suzuki, *Phys. Rev. B* **70**, 172108 (2004).
- G. N. Ruiz, L. E. Bove, H. R. Corti, and T. Loerting, *Phys. Chem. Chem. Phys.* **16**, 18553 (2014).
- F. Mallamace, C. Corsaro, D. Mallamace, C. Vasi, S. Vasi, and H. E. Stanley, *J. Chem. Phys.* **144**, 064506 (2016).
- L. Le and V. Molinero, *J. Phys. Chem. A* **115**, 5900 (2011).
- D. Corradini and P. Gallo, *J. Phys. Chem. B* **115**, 14161 (2011).
- D. A. Jahn, J. Wong, J. Bachler, T. Loerting, and N. Giovambattista, *Phys. Chem. Chem. Phys.* **18**, 11042 (2016).
- J. Bachler, V. Fuentes-Landete, D. A. Jahn, J. Wong, N. Giovambattista, and T. Loerting, *Phys. Chem. Chem. Phys.* **18**, 11058 (2016).
- I. Popov, A. Greenbaum (Gutina), A. P. Sokolov, and Y. Feldman, *Phys. Chem. Chem. Phys.* **17**, 18063 (2015).
- O. Andersson and A. Inaba, *J. Phys. Chem. Lett.* **3**, 1951 (2012).
- J. W. Biddle, V. Holten, and M. A. Anisimov, *J. Chem. Phys.* **141**, 074504 (2014).
- S. Chatterjee and P. G. Debenedetti, *J. Chem. Phys.* **124**, 154503 (2006).
- S. Woutersen, B. Ensing, M. Hilbers, Z. Zhao, and C. A. Angell, *Science* **359**, 1127 (2018).
- S.-H. Chen, L. Liu, E. Fratini, P. Baglioni, A. Faraone, and E. Mamontov, *Proc. Natl. Acad. Sci. U. S. A.* **103**, 9012 (2006).
- F. Mallamace, C. Corsaro, P. Baglioni, E. Fratini, and S.-H. Chen, *J. Phys.: Condens. Matter* **24**, 064103 (2012).
- F. Mallamace, P. Baglioni, C. Corsaro, S.-H. Chen, D. Mallamace, C. Vasi, and H. E. Stanley, *J. Chem. Phys.* **141**, 165104 (2014).
- Y. Yoshimura and H. Kanno, *J. Phys.: Condens. Matter* **14**, 10671 (2002).
- Y. Suzuki and O. Mishima, *Phys. Rev. Lett.* **85**, 1322 (2000).
- Y. Suzuki and O. Mishima, *J. Chem. Phys.* **138**, 084507 (2013).
- Y. Suzuki and Y. Tominaga, *J. Chem. Phys.* **134**, 244511 (2011).
- O. Mishima, *J. Chem. Phys.* **126**, 244507 (2007).
- A. Hauptmann, K. F. Handle, P. Baloh, H. Grothe, and T. Loerting, *J. Chem. Phys.* **145**, 211923 (2016).
- Y. Suzuki and O. Mishima, *J. Chem. Phys.* **117**, 1673 (2002).